Simultaneous Effects of Chemical Reaction, Heat Generation, Absorption on Solar Radiation over Magneto Hydrodynamics Stagnation Point Flow and Heat Transfer of a Nanofluid Over a Stretching Sheet

Abdullahi Madaki Gamsha[*], Abubakar Assidiq Hussaini[†], Amina Muhammad Musa[‡], Sanusi Kabiru Alaramma[§]

Abstract

This research is mainly concerned with the investigation of the influences of Heat generation/absorption as well as Chemical reaction over the MHD stagnation point flow along a stretchable sheet in a two- dimension. The effects of various physical parameters are considered such as Thermophoresis, solar radiation, Brownian motion, Magnetic field, among others. The governing system of partial differential equations is converted into an ordinary differential system by the use of boundary layer approximation alongside the similarity transformation which is then solved numerically by Runge-Kutta-Fehlberg method along with the shooting technique. The effects of these physical parameters are studied and analyzed using tables and graphs. The numerical results (validation tables) show the superb accuracy of our work when compared to the previous publications. Furthermore, it was discovered that temperature, nanoparticle concentration, Nusselt number also the thickness of the thermal boundary layer is rising functions with respect to heat generation/ absorption, chemical reaction, Eckert number and magnetic parameter, the data also revealed that when the chemical reaction parameter is increased this will result in a decrease of the Sherwood number, but the reverse is recorded in the case of heat generation/absorption parameter. Furthermore, momentum and nanoparticle concentration decrease rapidly with the increase in the values of radiation parameter.

***Keywords*:** Solar Radiation, heat generation/absorption, Chemical reaction, Nanofluid, Stretching surface

Introduction

Solar radiation, often known as solar resources or simply sunshine, is the electromagnetic energy emitted by the sun. Solar radiation may be captured and turned into useful electrical energy such as heat and electricity using a variety of methods. However, the technological

[*] Lecturer I (PhD), Department of Mathematical Sciences, Abubakar Tafawa Balewa University, PMB 0248, Bauchi. Nigeria, abdulmdk119@gmail.com.
[†] PG Scholar, Department of Mathematical Sciences, Abubakar Tafawa Balewa University, PMB 0248, Bauchi, Nigeria, alhajhabu@gmail.com.
[‡] Lecturer II, Aminu Saleh College of Education, PMB 044 Azare, Bauchi State, Nigeria, aminajao86@yahoo.com
[§] Lecturer II, Department of Mathematical Sciences, Abubakar Tafawa Balewa University, PMB 0248, Bauchi, Nigeria. sanusikabiratbu@yahoo.com

feasibility and purchase price among these systems in a specific location are dependent on solar resource availability. Solar energy is generally offered as perhaps the most promising source of renewable energy when all other activities have been completed in the country. Because of the important environmental issues and protective features, it is often considered that energy from the sun should have been employed besides other kinds, even if the ultimate prices were relatively increased Ghasemi et al (2013).

Humans have been gathering solar energy, or diffracted and heat of the sun, during earlier civilizations, utilizing variety of pace with the fast devices. Nasrin et al. (2012) Magnetohydrodynamics (MHD) can be considered as the intensity of a magnetic field on an electric conductivity of fluid's characteristics or management (or a combination of fluid dynamics and electromagnetism). Due to its thrust, numerous researches and manufacturing applications, including such electromagnetic blender, chemical reactions, MHD power generators, nuclear reactors, plasma education, aerodynamic and boundary layer control in the petroleum sector of the economy. MHD fluid flow has recently been the subject of a large number of studies. Abricka et al. (1997) Harada et al. (1998), Shang et al. (2001). The research for a better technique to increase the capabilities of the heat transfer rate has been a big essential issue in the industrial sphere in past few years. Energy transfer is fraught with problems, as heat-conducting materials fall short of industrialist expectations. The best technique to enhance thermal conductivity, according to the research, is to suspend nanoparticles with such a size of 100 nm. Nanofluid applications are critical in a variety of disciplines, including ventilation, conditioning systems, cooling systems, transportation, and nuclear applications. There are a lot of research outputs about nanofluids that govern flow and their different applications and uses. Mabood et al. (2015) used slip circumstances to express Magnetohydrodynamic nanofluid. To study melting as well as viscous dissipation, mathematical expressions have been used to guide the flux. He arrived at the conclusion that the magnitude of skin friction was reduced as a result of the administered magnetic force. Hag et al. (2016) investigated flow among two parallel plates separated by a finite distance.

The Cu-based nanoparticles are suspended in the fluid, and suction and injection effects are seen. The regulating flow effects of stretching permeability cylinder were discovered by Kishan et al. (2019). Curvature slip constraints are being used to sustain the Viscous incompressible nanoparticles. Prasannakumara et al. (2015) used partial derivatives to investigate the degradation of viscous as well as nanofluid interactions in governing equations. When compared to the present

outputs, there is a lot of agreement. Nadeem et al. (2020) discovered a stagnated flow of magnetized nanofluid due to a permeable stretching/shrinking surface with anisotropic slip.

For the Maxwell governing flow model, Madhu et al. (2017) described non-Newtonian fluid properties. The finite element approach is used to calculate the governing flow of unstable MHD. Palani et al. (2016) observed an increased chemical reaction in such an unstable UCM fluid, on the exponentially stretching sheet. The impacts of various dimensionless parameters flow are investigated. Circumventing nanoparticles were initially defined by Choi (1995), because their interaction increased thermophysical properties. Temperature distribution in the convection medium for nanofluids was addressed by Buongiorno (2006). On some kind of sheets, Vajravelu (1992) investigated Magnetohydrodynamic source of heat including thermal radiation. He defined non-Newtonian dominating gesture and linear order velocity with slope effects. Kakaç et al. (2019), Saleem et al. (2019), Nawaz et al. (2020), Hamad et al. (2019), Mair Khan et al. (2019), Sadiq et al. (2019), are a few notable investigations upon these fluids. As a result, several ways for enhancing the thermal resistivity of these fluids by embedding Nano-sized granular particles in liquids have indeed been developed.

Nanotechnology is widely used in industrial applications because nanometer-sized materials have unique chemical and physical capabilities. Choi et al. (2001), (2005) demonstrated that adding a minimal quantity of nanoparticles to standard heat transfer liquids (less than 1percent on average by volume) boosted the fluid's thermal conductivity to almost twice. Khanafer et al. (2003) carried out an investigation on the heat transfer mannerism of nanofluids inside the stockade, beguile taking into account dispersed nanoparticle. Numerous researchers are on the opinion that nanotechnology will metamorphose to be one of the foremost determinants driving the future major industrial transformation throughout these centuries, based on work of these researcher. The scientists used the simplest boundary conditions feasible, when both the temperature and the percentage of nanoparticles remains stable along the boundary. Nield and Kuznetsov (2009) also looked at the Cheng–Minkowycz (1977) problem of natural convection past a vertical plate in a porous media saturated with a nanofluid. The Brownian motion and thermophoresis characteristics are accounted for in the nanofluid concept. The Darcy model was used to simulate the porous structure.

The influence of a nanofluid beyond a stretchy cylinder in the applied magnetic field was investigated by Ghasemi et al. (2016) using the probative quadrature approach. Wubshet Ibrahim et al. (2016) investigated the impact of a magnetic intensity on stagnation point flow and thermal

growth from a nanofluid to stretching sheet. They used fourth-order Runge-Kutta method with shooting technique to solve the governing equations computationally. Nandeppanavar et al. (2017) explored an MHD stagnation point flow, mass and heat exchange through some kind of porous structure, and thermal radiation activity due to a porous stretched foil. The effects of thermal radiation and a non-uniform source of heat on Magnetohydrodynamic viscoelastic flow of fluids as well as heat transmission through a stretch foil were investigated by Subhas and Nandeppanavar et al. (2007).

Nandeppanavar et al. (2020) investigated the steady two-dimensional flow as well as boundaries, mass, and thermal expansion of non-Newtonian Casson nanofluids in the presence of an exponentially increasing layer. The magnetohydrodynamic heat and mass transport of three distinct nanofluids induced by a diminishing plate in a porous medium were numerically explored by Valipour and Ghasemi (2016). Ghasemi et al. (2021) used analytical and numerical simulations to assess Flow of blood in permeable arteries with Magnetohydrodynamic. Blood was seen as a non-Newtonian third-degree fluid containing nanoparticles by Mohammadian et al. (2015). The thickness of the velocity boundary layer grows as the volume fraction of nanoparticles increases, whereas the thickness of the thermal boundary layer declines. For two-dimensional nanofluids beneath two surfaces. Router et al. (2020) investigated the axisymmetric squeeze present Copper-water and copper-kerosene manifestations. They used the variational parameter strategy to address the complicated system of nonlinear equations analytically. The numerical investigation of radiative squeezing phenomena of fluid flows inside the Riga plate channels employing chemical process, heat source/sink Given boundary conditions that are convective was given by Thumma and Magagula (2020). To obtain the numerical results,

On the nonlinearly interconnected Ordinary differential equations that resulted, researchers employed the systemic localized linearization method (SLLM). Thumma et al. (2021) investigated the three-dimensional fluid motion in the presence of Lorentz force, Non-Newtonian Flow of fluid, thermal radiation, spontaneous movement of microscopic particles, and microscopic particle thermomigration due to temperature gradients all exist. as well as sources of heat using the generalized differential quadrature method (GDQM). Ghasemi et al. (2017) examined analytically and numerically the peristaltic flow of nanofluids in drug delivery systems, Wakif et al. (2021) proposed a fresh physical technique to solving the problem. Khader et al. (2013) investigated the thermo-magneto-hydrodynamic sustainability of a biphasic mixed hybridized nanofluid in a confined space with equivalent volumetric proportions of Aluminium

Oxide (Al_2O_3) and Cupper Oxide (CuO) nanoparticles in the liquefied stake. Thumma et al. (2017) explored the convective MHD mixed-transmission boundary-layer fluid wave of nanofluids past a nonlinearly flipped shrinking sheet in the light of viscous dissipation. They applied the method of Method Differential Transformation, the temperature profile in an appendage with temperature-dependent thermal conductivity and heat generation was explored by Ghasemi et al. (2014).

Thumma and Mishra (2020) investigated numerically the effect of non-uniform heat source/sink, viscosity, Joule dissipation on three dimensional Magnetohydrodynamic emanating Eyring-Powell flow of nanofluid through such an exponentially stretching exposed by slip effects, advection temperature, as well as zero mass flow rate boundary conditions, along with Joule dissipation on three dimensional Magnetohydrodynamic emitting Eyring-Powell flow of nanofluid through an extended surface exposed by slip effects, convection temperature, and zero mass flux boundary conditions. Naganthra et al. (2019) studied unrestricted convection in hydromagnetic boundary layer fluids flow pattern as well as thermal expansion through a vertical flat stretched sheet in a porous layer.

Predicated from the above momentary literature search, it is clear that to the best of the authors knowledge there has not been any research which considered the effects of these parameters on the current model. And hence, the main objective of this work is to apply the shooting technique and the method of Runge- Kutta- Fehlberg to productively tackle the MHD flow of nanofluids model across a stretching sheet taking into account chemical reaction and heat generation/absorption, moreover, the obtained results will then be compared with those published results such as Ghasemi et al. (2021), he, investigated the effects of solar radiation on MHD stagnation-point flow and heat transfer of a nanofluid over a stretching surface.

In addition, the influence of multiple critical parameters on nanoparticle concentration and temperature profiles is explored, encompassing the magnetic field parameters, thermal radiation, Prandtl number, thermophoresis and Brownian motion. In accordance with Mushtaq et al. (2014) and Nageeb et al. (2017) this same current study has several plausible implementations in the rectification, applied sciences, glass threads devise, as well as fusible substances processes that support cooling of lengthy strands or ribbons besides drawing them through still fluid, hardening and wave soldering of copper wires, and other processes where the characteristics of the melting point seems to have a significant impact on the final result.

Mathematical analysis

We investigate the velocity distribution of the equation uw (x) = ax for a continuous two-dimensional boundary layer flow of a nanofluid where a is constant. in the presence of a chemical reaction and heat generation/absorption via solar radiation, as illustrated on Fig1. It is believed that a magnetic field of constant strength exists. In orientations where the material is spread horizontally between the x and y axes, the forces are equal and opposed from the origin. For a length of x, where uw = ax and an is larger than 0, the speed at the base of the coating is kept constant, where x denotes the sheet dimension and the surface velocity remain constant. The fluid's free stream velocity is given by U(x) = bx. Longitudinal magnetic parameter becomes afflicted to passage at y greater than 0, that is orthogonal towards the orientation of fluid velocity. assuming that both the charge polarization-induced electrical field and the external electrical field are minimal. The impacts of chemical reactions, heat generation and absorption, and other relevant features are then taken into account during a mass transfer study.

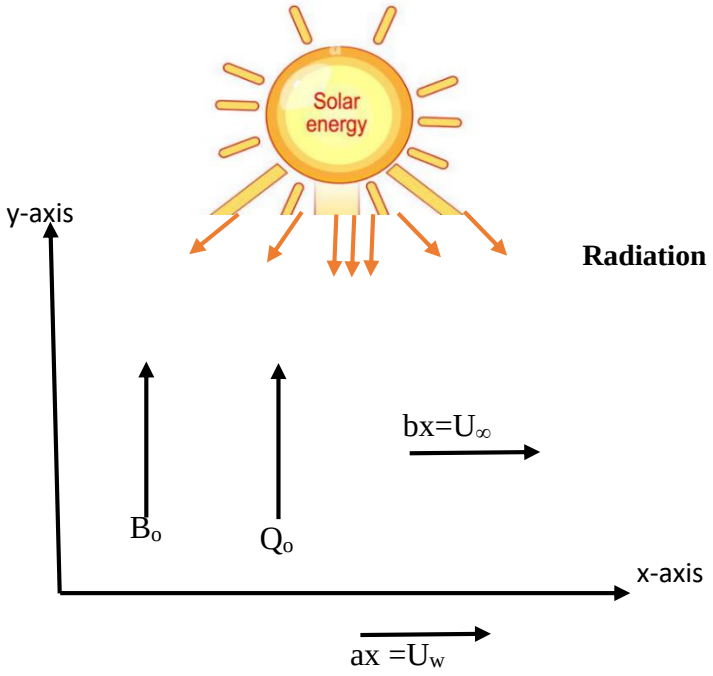

Figure 1: The flow model

For the conservation of mass, momentum, temperature, and nanoparticle concentration, these would be the governing equations. after addition of chemical reaction as well as heat generation/absorption as in Ghasemi et al. (2021):

$$\frac{\partial u}{\partial x}+\frac{\partial u}{\partial y}=0 \qquad \ldots \quad (1).$$

$$u\frac{\partial u}{\partial x}+v\frac{\partial u}{\partial y}=U_{\infty}\frac{du_{\infty}}{\partial x}+\nu_f\frac{\partial^2 u}{\partial x^2}-\frac{\sigma_e B_0^2}{\rho_f}(u-u_{\infty}) \qquad \ldots \quad (2).$$

$$u\frac{\partial T}{\partial x}+v\frac{\partial T}{\partial y}=\frac{Q}{\rho_{nf}}(T-T_{\infty})+\alpha\frac{\partial^2 T}{\partial y^2}+\frac{\sigma_e B_0^2}{(\rho C)_f}(u_{\infty}-u)^2\frac{\nu_f}{C_f}\left(\frac{\partial u}{\partial y}\right)^2$$

$$+\tau D_B\left[\frac{\partial T}{\partial y}\frac{\partial C}{\partial y}+\frac{D_T}{T_{\infty}}\left(\frac{\partial T}{\partial y}\right)^2\right]-\frac{1}{(\rho C)_f}\left(\frac{\partial q_r}{\partial y}\right) \qquad \ldots \quad (3).$$

$$u\frac{\partial C}{\partial y}+v\frac{\partial C}{\partial y}=D_B\frac{\partial^2 C}{\partial y^2}+\frac{D_T}{T_{\infty}}\frac{\partial^2 T}{\partial y^2}+k_1(C-C_{\infty}) \qquad \ldots \quad (4)$$

in which ν_f stands for kinematic viscosity, σ_e for fluid electrical conductivity, B_0 for a homogeneous magnetic field along the y-axis, D_B Brownian diffusion coefficient, k thermal conductivity of base fluid, α is thermal diffusivity of the base fluid, D_T thermophoretic diffusion coefficient, u and v for velocity components in the x -axis and y -axis, T is the temperature and C is the concentration. Q the heat generation/absorption coefficient and $\tau=\frac{(\rho C)_p}{(\rho C)_f}$, refers for the ratio of the heat capacity of the base fluid to the effective heat capacity of the nanoparticles, ρ_f density of base fluid, $(\rho C)_f$ heat capacity of the base fluid, $(\rho C)_p$ heat capacity of the nanoparticle material, T_{∞} ambient temperature whereby q_r represents for the amount of radiative heat flux. The Rosseland approximation for thermal radiation can be used to compute the radiative heat flux and extended to optically thick surfaces. as well as [Brewster (1972), Raptis (1998) and Sparrow (1978)].

$$q_r=\frac{16\sigma^*}{3k^*}T^3\frac{\partial T}{\partial y}=-\frac{4\sigma^*}{3k^*}\frac{\partial T^4}{\partial y} \qquad \ldots \quad (5).$$

The notation for the Stefan-Boltzmann constant and mean absorption coefficient are σ^* and k^*, respectively. Relying upon previous research [Mushtaq et al. (2014)], Radiative heat flux modeling uses the

nonlinear Rosseland approximations [Ghasemi et al. (2016), Ghasemi et al. (2021)]. The pertinent heat transfer by convection boundary conditions can be expressed as follows

$$when\ y = 0 : C = C_w, -k\frac{\partial T}{\partial y} = h(T - T_f)$$

$$when\ y \to \infty : C \to C_\infty, T \to T_{\infty,} \quad \ldots \quad (6).$$

Additionally, as in Ghasemi et al. (2021), the accompanying non - dimensional quantities

$$u = axf'(\eta),\ v = -\sqrt{av_f}\, f(\eta),\ \eta = \sqrt{\frac{a}{v_f}}\, y, \quad \ldots \quad (7).$$

The entire first portion at the right-hand side of Eq. (2) would then be transcribed to $\alpha\frac{\partial}{\partial y}\left[\frac{\partial T}{\partial y}\left(1 + R_d(\theta_w - 1)\theta^3\right)\right], where\ \ R_d = 16\sigma^* T_\infty^3 / 3kk^*$ the non-dimensional temperature profile can now be defined as R_d=0, with $T = T_\infty\left(1 + (\theta_w - 1)\theta\right)$ and $\theta(\eta) = T - T_\infty / T_f$ is the scenario when there is no thermal radiation impact.

The last statement can also be simplified to $\frac{\alpha(T_f - T_\infty)}{\Pr}\left[\left(1 + R_d\left(1 + (\theta_w - 1)\theta^3\right)\theta'\right)\right]'$, Pr: the Prandtl number, which is expressed as $\Pr = v_f / \alpha$.

By introducing the boundary conditions eq. (6) as well as the dimensionless quantities in eq. (7). Equation (1) is satisfied automatically, whereas, eq. (2), eq. (3) and eq. (4) constitute these ODEs:

$$f''' + ff'' - f'^2 + A^2 + M(A - f') = 0 \quad \ldots \quad (8).$$

$$\frac{1}{\Pr}\left[\left(1 + R_d\left\{1 + (\theta_w - 1)\theta\right\}^3\right)\theta'\right]' + MEc\left(A - f'\right)^2 + N_b\,\theta'\varphi' + \lambda\theta$$

$$+ N_t\theta'^2 + E_c f''^2 + f\,\theta' = 0 \quad \ldots \quad (9).$$

$$\varphi'' + \frac{N_t}{N_b}\theta'' - \gamma\varphi + Lef\varphi' = 0 \quad \ldots \quad (10).$$

Moreover, if A=0, the precise solution of Eq (5) may be determined by using where T is the temperature, C is the concentration of nanoparticles, is the fluid's specific heat, and are the Brownian motion and thermophoretic diffusion coefficients, respectively.

Additionally, if A=0, it is possible to calculate the accurate solution of Eq (5) by using $f = (1-e^{-\sqrt{1+M}\eta})/\sqrt{1+M}$, where T, C, C_f, D_B and D_T are the temperature, concentration of nanoparticles, fluid's specific heat, the Brownian motion and thermophoretic diffusion coefficients respectively. Throughout this study, prime denotes the function's differentiation with respect to $\eta, while\ M = \frac{\sigma_e B_0^2}{a\rho_f}, A = \frac{b}{a}$ are the magnetic parameter and correlation of free stream velocity versus stretched sheet velocity, and $\lambda = \frac{Q}{aT_w\rho_{nf}}$ would be the heat generation/absorption parameter. The following boundary conditions apply to Equations (8) – (10):

$$f(0)=0,\ f'(0)=1,\ f'(\infty)=A,\ \theta(\infty)=0,,\ \theta'(0)=-Bi[1-\theta(0)],\varphi(0)=1,$$
$$\varphi(\infty)=0 \quad \ldots \quad (11).$$

The following are among the system parameters throughout Equations. (8)– (10):

$$Bi=\frac{h(v_f/a)^{1/2}}{k}, Le=\frac{v_f}{D_B},\ Nt=\frac{\tau D_B(T_f-T_\infty)}{v_f T_\infty},\ Nb=\frac{\tau D_B(C_w-C_\infty)}{v_f},$$

$$Ec=\frac{U_w^2(x)}{C_n(T_w-T_\infty)}, \gamma=\frac{k_1 v_f(C_w-C_\infty)}{aD_B C_w}, \varphi(\eta)=C-C_\infty/C_w-C_\infty.$$

The chemical reaction parameter is λ, the Brownian motion parameter is Nb, the thermophoresis parameter is Nt, the Biot number is Bi, the Eckert number is Ec, and the Lewis number is Le. Nusselt's number is Nu, and the Sherwood number, Sh, are the quantities of practical interest. As previously stated, the x-coordinate fails to apt into the energy equation. Correspondingly, the authors attempt for the most restricted similarity solutions conceivable. The wall mass flux, heat flux represented by q_m and q_w respectively which are supplied as follows:

$$q_w = -k\left(\frac{\partial T}{\partial y}\right)_{y=0} + (q_r)_w = -k(T_w-T_\infty)(a/v_f)^{1/2}[1+N\theta_c^3]\theta'(0),$$

$$q_m = -D_B\left(\frac{\partial C}{\partial y}\right)_{y=0} = -D_B(C_w-C_\infty)(a/v_f)^{1/2}\varphi'(0). \quad \ldots \quad (12).$$

By introducing the Nusselt number $Nu_x = xq_w/k(T_f-T_\infty)$ and local Sherwood number $Sh = xq_m/D_B(C_w-C_\infty)$ and the relation becomes

$$Nur = \frac{Nu_x}{\sqrt{\mathrm{Re}_x}} = -[1 + R_d\theta_w^3]\theta'(0),\ Shr = \frac{Sh}{\sqrt{\mathrm{Re}_x}} - \varphi'(0) \quad \ldots \quad (13).$$

Thus, $\mathrm{Re}_x = u_w(x)/\nu$ stands for the nanofluid's local Reynolds number throughout this analysis.

Result and Discussion

This section shows how we visualized the influences of crucial as well as relevant variables for the velocity profile, temperature profile, nanoparticle concentration, as well as Nusselt number and Sherwood number. The schematic of the flow for the aforementioned non-linearly ordinary differential equations (ODEs) Eqs. (8) – (10) was solved using an efficient fourth order Runge–Kutta method and a shot methodology. With respect to their boundary conditions. heat generation/absorption parameter (γ), Prandtl number (Pr), Brownian motion parameter (Nb), radiation parameter (Rd), thermophoresis parameter (Nt), chemical reaction parameter (λ), Lewis number (Le) and magnetic parameter (M), among others, constituted the governing parameters of the model. For varying priorities of the relevant parameters, numerical results for the Nusselt number, the Sherwood number, velocity, temperature, and concentration profiles are constructed.

Figs 2–19 displayed the accumulated reports for the momentum profile, energy profile, the Nusselt number profile, the Sherwood number profile, as well as the nanoparticle concentration profile. 1st table and 2nd table show the precision of our results for various values of the governing factors involved in the model for Nusselt number and Sherwood number respectively, when chemical reaction as well as the Heat generation/absorption parameters are nullified. As a result, there was a fascinating agreement between the current and past investigations.

Table 1
Comparison table for the Nusselt number

N_b	Ghasemi et al. (2021)	Present Study	Error
0.1	0.9524	0.9526	0.0002
0.2	0.5056	0.5056	0.0000
0.3	0.2522	0.2524	0.0002
0.4	0.1194	0.1198	0.0004
0.5	0.0543	0.0545	0.0002

Table 2
Comparison table for the Sherwood number (-φ'(0)), when Pr=10, Nb =0.1, Le=10, Rd =1

N_t	Ghasemi et al. (2021)	Present Study	Error
0.1	2.1295	2.1295	0.0000
0.2	2.2744	2.2747	0.0003
0.3	2.5288	2.5288	0.0000
0.4	2.7955	2.7957	0.0002
0.5	3.0353	3.0353	0.0000

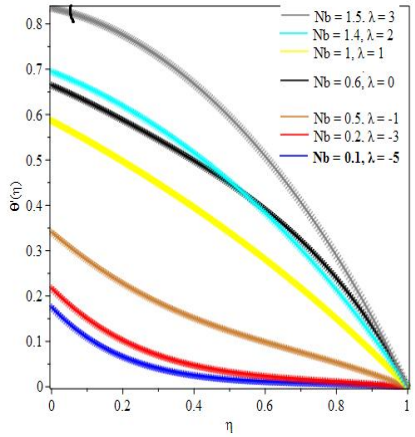

Figure 2: Effects of Brownian motion and heat generation/absorption on temperature profile

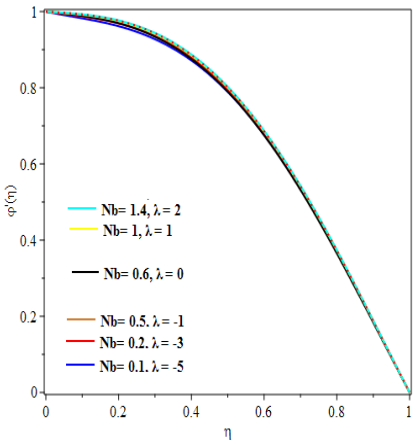

Figure 3: Effects of Brownian motion and heat generation/absorption on concentration

Analysis of Brownian motion parameter (Nb) alongside heat generation/absorption parameter on the distribution of temperature profile, nanoparticle concentration profile is displayed in figure2 and figure3 respectively, increment in heat generation ($\lambda > 0$) parameter as well as heat absorption parameter ($\lambda < 0$) increases the temperature field. Nanoparticle concentration

profile also displayed increasing behavior for any increase of heat generation parameter as well as an increase in the heat absorption parameter.

Figures 4 and 5 show the variation of temperature and concentration profiles as a function of chemical reaction parameter and Eckert number. It has been discovered that increasing the value of the chemical reaction parameter in conjunction with the Eckert number raises the temperature. On the one hand, increasing the chemical reaction parameter alongside the Eckert number increases the concentration of species in the boundary layer; on the other hand, increasing the chemical reaction parameter has no effect on the fluid velocity. This is because the chemical reaction in this system causes the chemical to be consumed, resulting in a rise in the concentration profile. The most significant consequence is that the first order chemical reaction tends to reduce overshoot in the profiles of the variables.

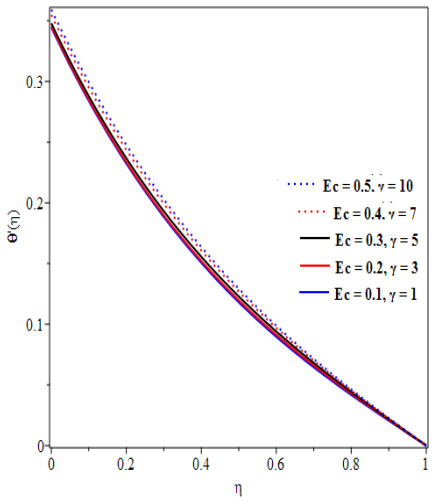

Figure 4: Effects of Eckert number and chemical reaction on temperature

An influence by chemical reaction parameter, as well as magnetic parameter, on momentum, temperature, and concentration profiles is depicted in Figures 6, 7, and 8 respectively. It has been noticed that when both parameters are increased, the momentum profile increases. For increasing levels of both the chemical reaction and the magnetic parameter, the temperature profile and the concentration profile both increases. This is because, when chemical reaction exists, increasing the Magnetic Parameter M reduces the boundary layer thickness and increases the heat transfer rate on the melting surface.

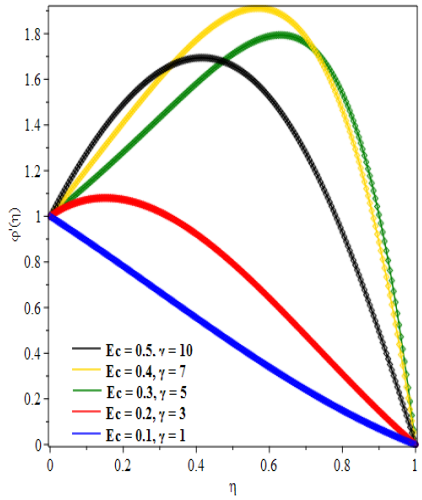

Figure 5: Effects of Eckert number and chemical reaction parameter on nanoparticle concentration profile

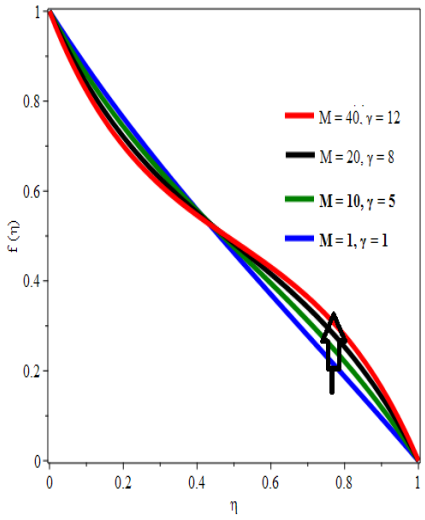

Figure 6: Effects of Magnetic Parameter and Chemical reaction parameter on Momentum profile

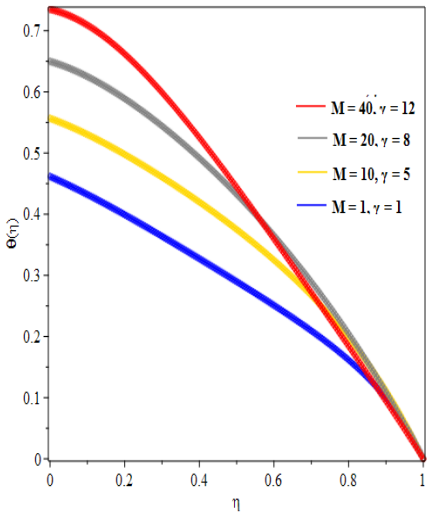

Figure 7: Effects of Magnetic Parameter and Chemical Reaction Parameter on Temperature

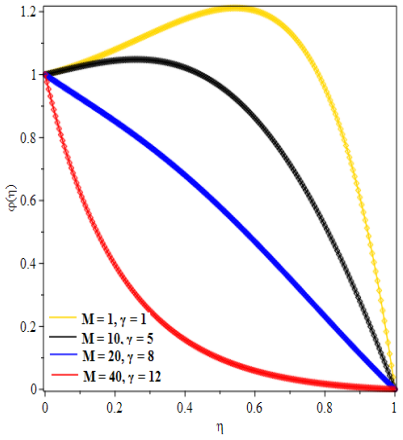

Figure 8: Effects of Magnetic parameter and Chemical reaction on temperature profile

Figures 9 and 10 show the effect of Lewis number (Le) and chemical reaction parameter (γ) on temperature and concentration profiles. In the presence of Lewis number, the temperature profile obviously increases with an increase in the chemical reaction parameter. The volume fraction of nanoparticles increases as both parameters increase, and the thickness of the boundary layer grows significantly as Le increases.

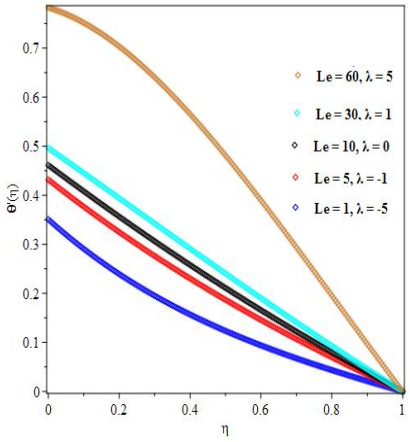

Figure 9: Effects of Lewis number and heat gen./abs parameter on concentration profile

The influence of the radiation parameter on momentum, temperature, and concentration profiles is depicted in Figures 11, 12, and 13 respectively. It is noticed that when the value of the radiation parameter increases, the momentum and concentration profiles decrease, but the temperature profile increases. This is because, in the presence of a magnetic parameter, increasing the radiation parameter R reduces the boundary layer thickness and increases the heat transfer rate on the melting surface.

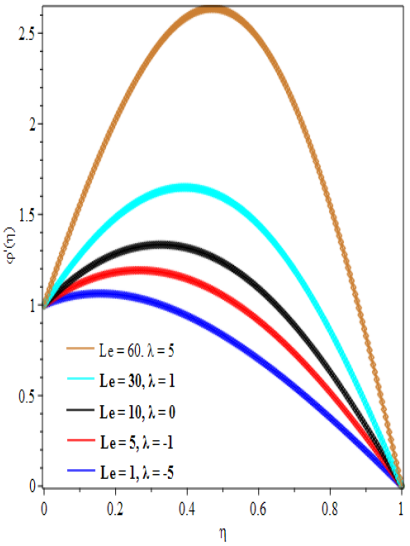

Figure 10: Effects of Lewis number and heat generation/absorption on nanoparticle concentration profile.

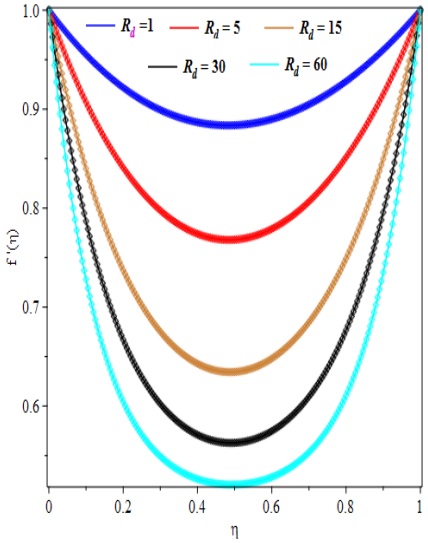

Figure 11: Effects of Radiation parameter (R_d) and magnetic parameter (M=1,5,15,30,60) on momentum profile.

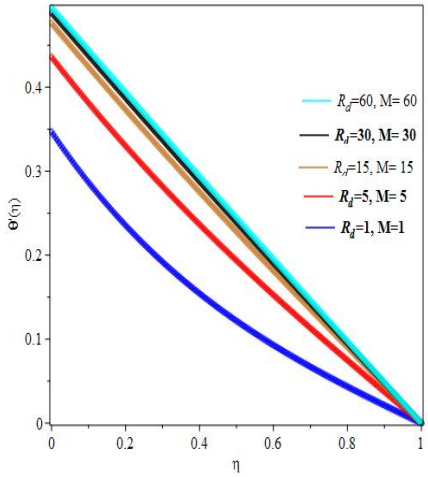

Figure 12: Effects of Radiation parameter and Magnetic parameter on Temperature profile

Figures 14 and 15 shows the effects of the thermophoresis parameter on the Nusselt number and Sherwood number profiles, demonstrating that an increase in the thermophoretic parameter results in a larger Nusselt number, Greater Nt results in a larger Nusselt number differential and shear variation in the profiles, as expected. Another meta-analysis is the impacts of thermophoresis, based on Ghasemi et al. (2021), indicates that a variety of reactions to a Nusselt number gradient's force are adequate to increase Nusselt

number dispersion resulting in increased thermophoresis. Reverse of this case is recorded as for the Sherwood number profile, fig. 15.

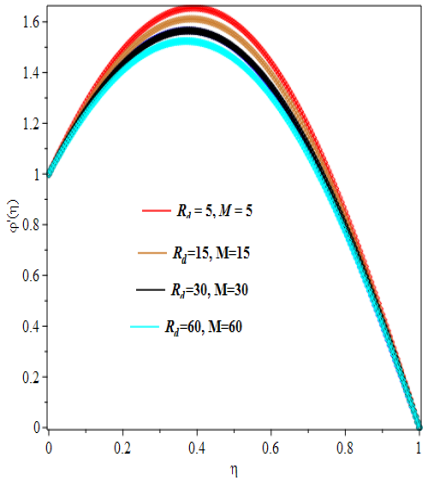

Figure 13: Effects of Radiation parameter and Magnetic parameter on concentration profile

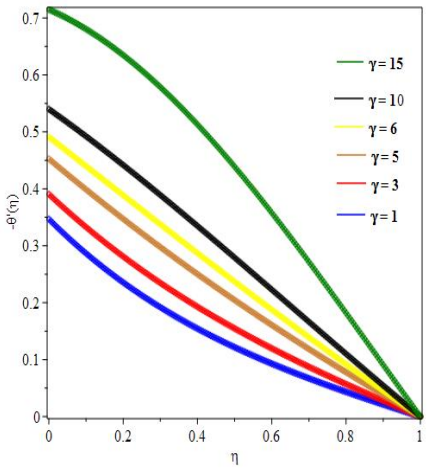

Figure 14: effects of chemical reaction and thermophoresis (Nt= -0.9, -0.5, -0.1, 0, 1, 2) on Nusselt number profile.

Figure 16 depicts the characteristics of the heat generation/absorption parameter on the Nusselt number profile in the presence of magnetic parameter. When the heat generation parameter ($\lambda > 0$) is increased, the Nusselt number grows, and with regard to heat absorption parameter ($\lambda < 0$) increment, reverse is the case. As the heat generation parameter increases, the Nusselt number profile and the thickness of the thermal boundary layer both increases. More heat is produced as a result of a higher heat generation parameter, which improves the Nusselt number field.

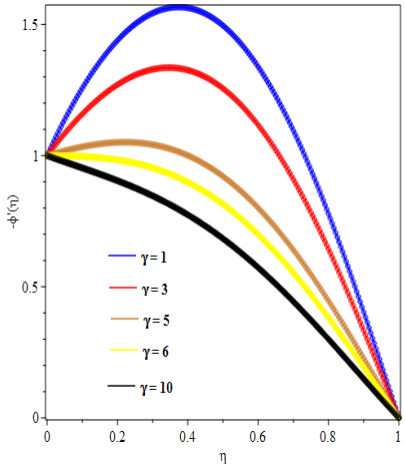

Figure 15: effects of chemical reaction and thermophoresis on Sherwood number profile

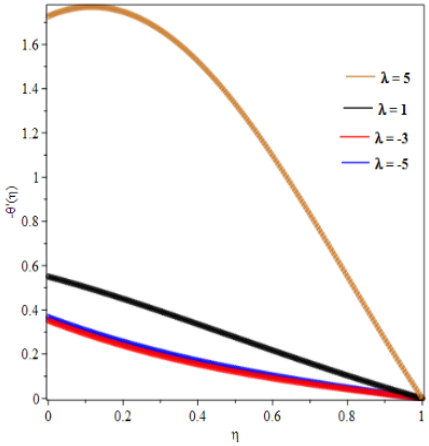

Figure16: effects of heat generation/absorption on the Nusselt number Profile, when Pr=1, 5, 10, 15.

An influence of heat generation/absorption parameter to Sherwood number is displayed on figure 17, in both cases of either heat generation/absorption increase in the parameter values increase the Sherwood number. Furthermore, it can be clearly observed on figures 18 and 19, the effects of Prandtl number on Nusselt number and Sherwood number profiles respectively. Increase in the values of Prandtl number decrease the Nusselt number, and reverse is the case for the Sherwood number.

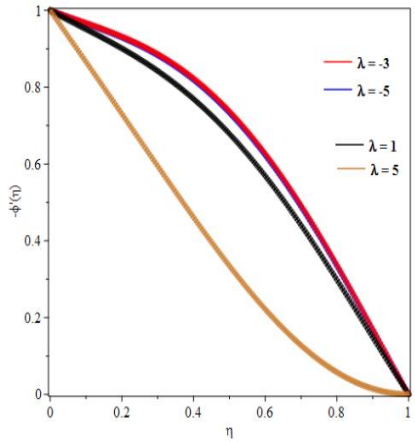

Figure 17: Effects of heat generation/absorption on the Sherwood number Profile, along Pr.

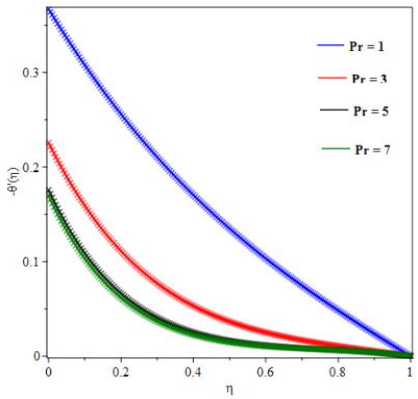

Figure 18: Effects of Prandtl number on Sherwood number Profile

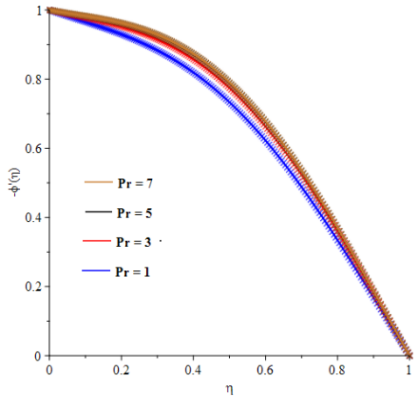

Figure 19: Effects of Prandtl number on Nusselt number profile

Conclusion

We investigated slip flow and heat transfer in the vicinity of a nanofluid's stagnation point in the presence of chemical reaction and heat generation/absorption on a stretching sheet.

1. The governing equations of the problem are translated into ordinary differential equations using appropriate similarity transformations.
2. The fourth order Runge–Kutta method with shooting technique is used to solve the similarity equations numerically.
3. The results of this work are in good accord with those of earlier studies; momentum, temperature, nanoparticle concentration profiles, as well as Nusselt and Sherwood numbers, are all heavily influenced by the parameters. The acquired data are represented graphically and in tables to show the impact of various physical parameters on velocity components and temperature. and concentration profiles, as well as the Nusselt and Sherwood numbers thus
    i. Increase in the heat generation/ absorption parameter produces an increase in the temperature and concentration profiles
    ii. Dual increments in the Eckert number and chemical reaction parameters yield increase in temperature and concentration profiles, while keeping the momentum profile constant
    iii. Whenever there is an increase in the chemical reaction parameter along magnetic field this produces increment in both temperature and concentration profiles.
    iv. Likewise, similar result as (iii) is experienced in the case of Lewis number along chemical reaction parameter.
    v. For any increase in thermophoresis parameter (Nt) increases the Nusselt number but reduces the Sherwood number.
    vi. Heat generation along with magnetic field increases the Nusselt number, reverse is the case for Sherwood number.
    vii. Irrespective of heat generation/ absorption, increase the parameter produces an increase in the Sherwood number.
    viii. When Prandtl number is increased, an increased in observed on the Sherwood number while reverse is the case for Nusselt number.

References

Abricka, M., Krumin˘s, J. & Gelfgat, Yu. (1997). Numerical simulation of MHD rotator action on hydrodynamics and heat transport in single crystal growth processes, *J. Cryst. Growth.* 180, 388–400.

Bellman, R.E., Kashef, B.G. & J. Casti, (1972). Differential quadrature: a technique for the rapid solution of nonlinear partial differential equations, *J. Comput. Phys.* 10, 40–52.

Choi, S.U.S. (1995). Enhancing thermal conductivity of fluids with nanoparticles, in: The Proceedings of the ASME International Mechanical Engineering Congress and Exposition, *San Francisco, USA, ASME, FED 231/MD*, 66, 99–105.

Choi, S.U.S., Zhang, Z.G., Yu, W., Lockwood, F.E. & Grulke, E.A. (2001).

Anomalously thermal conductivity enhancement in nanotube suspensions, *Appl. Phys. Lett.* 79, 2252–2254.

Cheng, P. & Minkowycz, W.J. (1977). Free convection about a vertical flat plate embedded in a porous medium with application to heat transfer from a dike, *J. Geophys. Res.* 82, 2040– 2044.

Darzi, M., Vatani, M., Ghasemi, S.E., & Ganji, D.D. (2015). Effect of thermal radiation on velocity and temperature fields of a thin liquid film over a stretching sheet in a porous medium, *Eur. Phys. J. Plus.* 130 (100), 2-11.

Ghasemi, S.E., Zolfagharian, A., Hatami, M. & Ganji, D.D. (2016). Analytical thermal study on nonlinear fundamental heat transfer cases using a novel computational technique, *Applied Thermal Engineering*, *Appl. Therm. Eng.* 98, 88–97,

Ghasemi, S.E., Hatami, M., Hatami, J., Sahebi, S.A.R. & Ganji, D.D. (2016). An efficient approach to study the pulsatile blood flow in femoral and coronary arteries by Differential Quadrature Method, *Physica A.* 443, 406–414.

Ghasemi, S.E., Hatami, M., Salarian, Armia & Domairry, G. (2016). Thermal and fluid analysis on effects of a nanofluid outside of a stretching cylinder with magnetic field the using differential quadrature method, J. *Theor. Appl. Mech.* 54 (2), 517–528.

Harada, N. & Tsunoda, K. (1998). Study of a disk MHD generator for non-equilibrium plasma generator (NPG) system, *Energy Convers. Manag.* 39, 493–503.

Hussaini, A. A., Madaki, A.G. & Kwami A.M. (2021). Modified Mathematical Model on the Study of Convective MHD Nanofluid flow with Heat Generation/Absorption, *Int. J. Engineering research and technology*. 10 (09), 155- 163.

Hussaini, A. A, Madaki, A. G., Alaramma, S.K. & A. Barde, (2022). Numerical Study on the Influence of Thermophores and Magnetic Field on the Boundary Layer Flow Over a Moving Surface in a Nanofluid, *Int. J. Scientific Research and Modern Technology.* 2 (1), 4- 9.

Ibrahim, Wubshet, Shankar, Bandari, Mahantesh M. & Nandeppanavar. (2013). MHD stagnation point flow and heat transfer due to nanofluid towards a stretching sheet, *Int. J. Heat Mass Tran*. 56 (1–2), 1–9.

Jawad, M., Shah, Z., Islam, S., Khan, W. & Khan, A.Z. (2019). Nanofluid thin film flow of Sisko fluid and variable heat transfer over an unsteady stretching surface with external magnetic field, *J. Algorithm Comput. Technol.* 13, 1 to 16.

Kakaç, S., & Pramuanjaroenkij, A. (2009). Review of convective heat transfer enhancement with nanofluids, *Int. J. Heat Mass Transfer.* 52, 3187–3196.

Khanafer, K., Vafai, K. & Lightstone, M. (2003). Buoyancy-driven heat transfer enhancement in a two-dimensional enclosure utilizing nanofluids, *Int. J. Heat Mass Transfer.* 46, 3639–3653.

Kang, H.U., Kim, S.H. Oh, & J.M. (2006). Estimation of thermal conductivity of

nanofluid using experimental effective particle volume, *Exp. Heat Transfer*, 19, 181–191.

Khan, W. A., Pop I. (2010). Boundary-layer flow of a nanofluid past a stretching Sheet, *Int. J. Heat Mass Transfer*. 53, 2477–2483.

Khan, W.A. & Pop, I. (2010). Boundary-layer flow of a nanofluid past a stretching Sheet, *Int. J. Heat Mass Tran.* 53, 2477 to 2483.

Mahantesh M., Nandeppanavar, M., Abel, Subhas & Kemparaju, M.C. (2017). Stagnation point flow, heat and mass transfer of MHD nanofluid due to porous stretching sheet through porous media with effect of thermal radiation, *Journal of Nanofluids.* 6 (1), 38–47.

Madaki, A. G., Yakubu, D. G., Adamu, M. Y., & Roslan, R. (2019). The study of MHD Nanofluid flow with chemical reaction along with thermophoresis and Brownian motion on boundary layer flow over a linearly stretching sheet, *J. of pure and applied sci. 19, 83 – 91*

Madaki, A.G., Roslan, R., Rusiman, M.S., Raju C.S.K. (2018). Analytical and numerical solutions of squeezing unsteady Cu and TiO2-nanofluid flow in the presence of thermal radiation and heat generation/absorption, *Alexandria Engineering J., 57, 1033-1040*

Mahantesh M., Nandeppanavar, S., Vaishali, M.C., Kemparaju, N. & Raveendra. (2020). Theoretical analysis of thermal characteristics of casson nano fluid flow past an exponential stretching sheet in Darcy porous media, *Case Studies in Thermal Engineering.* 21, 100717.

Maiga, S.E.B., Palm, S.J., Nguyen, C.T., Roy, G. & Galanis, N. (2005), Heat transfer enhancement by using nanofluids in forced convection flow, *Int. J. Heat Fluid Flow.* 26, 530–546.

Moghimi, M.A., Tabaei, H., & Kimiaeifar, A. (2013). HAM and DQM solutions for slip flow over a flat plate in the presence of constant heat flux, *Math. Comput. Model.* 58, 1704–1713.

Moghimi, M.A., Talebizadeh, P. & Mehrabian, M.A. (2011). Heat generation/absorption effects on magnetohydrodynamic natural convection flow over a sphere in a non- Darcian porous medium, *Proc. IME E J. Process Mech. Eng.* 225, 29–39.

Nasrin, R. & Alim, M.A. (2012). Dufour-soret effects on natural convection inside a solar collector utilizing water-cuo nanofluid, *Int. J.* Energy *& Technology*. 4 (23) 1–10.

Nield, D.A. & Kuznetsov, A.V. (2009). The Cheng-Minkowycz problem for natural convective boundary layer flow in a porous medium saturated by a nanofluid, *Int. J. Heat Mass Transfer*. 52, 5792–5795.

Shang, J.S. (2001). Recent research in magneto-aerodynamics, *Prog. Aero. Sci.* 37, 1–20.

Shu, C. (2012). Differential Quadrature and its Application in Engineering, *Springer*.

Subhas M., Abel, & Nandeppanavar, M.M. (2007). Effects of thermal radiation and non-uniform heat source on MHD flow of viscoelastic fluid and heat transfer over a stretching sheet, *Int. J. Appl. Mech. Eng.* 12 (4), 903–918.

Talebizadeh, P., Moghimi, M.A., Kimiaeifar, A. & Ameri, M. (2011). Numerical and analytical solution for natural convection flow with thermal radiation and mass transfer past a moving vertical porous plate by DQM and HAM, *Int. J. Comput. Methods.* 8, 611–631.

Valipour, P., Ghasemi, S.E. (2016). Numerical investigation of MHD water-based nanofluids flow in porous medium caused by shrinking permeable sheet, *J. Braz. Soc. Mech. Sci. Eng*. 38, 859–868.

Wang, C.Y. (1989). Free convection on a vertical stretching surface, *J. Appl. Math. Mech. (ZAMM).* 69, 418–420.